Pharm Res (2015) 32:3137–3148
DOI 10.1007/s11095-015-1677-3

RESEARCH PAPER

Dual Drug Delivery Using Lactic Acid Conjugated SLN for Effective Management of Neurocysticercosis

Rekha Devi[1] • Ankit Jain[1] • Pooja Hurkat[1] • Sanjay K. Jain[1]

Received: 1 December 2014 / Accepted: 10 March 2015 / Published online: 22 July 2015

ABSTRACT

Purpose The debut study was aimed to develop Lactic acid (LA)-conjugated solid lipid nanoparticles (SLN-LA) bearing albendazole (ALB) and prednisolone (PRD) for effective management of neurocysticercosis (NCC).

Methods LA was coupled to SLN by post-insertion technique. SLNs were characterized for particle size and size distribution, shape, and percent drug entrapment efficiency. *In vitro* drug release kinetics, fluorescence study and *in vitro* transendothelial transport, hematological studies and pharmacokinetic studies were carried out to predict the fullest drug delivery potential.

Results Spherical SLNs (~100 nm) with good drug entrapments (~64 and ~78% for ALB and PRD, respectively) showed *in vitro* initial fast release (i.e., 20–40% drugs release in 4 h) followed by sustained release for more than 48 h. Fluorescence study and *in vitro* transendothelial transport depicted selective brain uptake of SLN-LA compared to SLN attributed to carrier mediated transport via monocarboxylic acid transporters (MCT – 1/2/3). Pharmacokinetic parameters such as $AUC_{0\text{-}t}$ and $AUMC_{0\text{-}t}$ and Cl_{last} showed good drugs withholding capacity of SLNs. Organ distribution studies reflected high accumulation of drugs (ALB, 7.6 ± 0.31%; PRD, 5.21 ± 0.24%) in the brain after 24 h in case of SLN-LA as compared to plain drugs solution. SLN-LA in hematological studies revealed insignificant toxicity to blood cells.

Conclusions The overall study paved the potential advances in brain targeting with synergistic acting drugs for effective management of NCC.

✉ Sanjay K. Jain
drskjainin@yahoo.com

[1] Pharmaceutics Research Projects Laboratory, Department of Pharmaceutical Sciences, Dr. Hari Singh Gour Vishwavidyalaya Sagar, (M.P.) 470 003, India

KEY WORDS albendazole · lactic acid · neurocysticercosis · prednisolone · solid lipid nanoparticles

ABBREVIATIONS

%EE	Percent entrapment efficiency
ACs	Astrocyte cells
ALB	Albendazole
BBB	Blood brain barrier
BCECs	Brain capillary endothelial cells
BCRP	Breast cancer resistance protein
CMT	Carrier mediated transporters
DDW	Double distilled water
EDC	1-ethyl-3-(3-dimethylaminopropyl) carbodiimide
FITC	Fluorescein isothiocyanate
Hb	Hemoglobin
HSPC	Hydrogenated soya phosphatidylcholine
LA	DL-lactic acid
MCT	Monocarboxylic acid transporters
MRP	Multidrug resistance proteins
NCC	Neurocysticercosis
OLA	OH protected LA
P-gp	P-glycoprotein
PRD	Prednisolone
RBC	Red blood corpuscles
SA	Stearylamine
SD	Standard deviation
SLN-LA	Lactic acid conjugated SLN loaded with ALB-PRD
SLNs	Solid lipid nanoparticles
Sulfo-NHS	N-Hydroxysulfosuccinimide
WBC	White blood corpuscles
XRD	X-ray diffraction

INTRODUCTION

Neurocysticercosis (NCC) is a primary infection of the brain, spinal cord or peri-meningeal structures with the larval forms of *Taenia solium* and the associated inflammation, which is even aggravated due to the debris of parasites by the anthelminthics (1, 2). In addition, the treatment or management faces many barriers such as blood brain barrier (BBB) which disallows most of the molecules to enter the brain. BBB being highly lipoidal is endowed with endothelial cells with tight junction, enzymatic activity and the presence of active efflux transport mechanisms like P-glycoprotein (P-gp) efflux (3, 4). To convey nutrients, brain contains various carrier mediated transporters (CMT) such as monocarboxylic acid transporters (MCT) responsible for transport of monocarboxylic acids i.e., lactic acid, pyruvic acid and ketoacids etc. (5, 6). Treatment of NCC must be tailored to deliver anthelminthics like Albendazole (ALB) and corticosteroids like Prednisolone (PRD) leading to synergistic pharmacologic manifestations (7). ALB kills the cysts and parasites in the brain and PRD alleviates inflammation caused by the dead parasites (8, 9). Lipidic nanocarriers like solid lipid nanoparticles (SLNs) are found to permeate across BBB (10) as small hydrophobic entities of 400–600 D can diffuse passively across the BBB into the brain but get exposed to efflux pumps such as P-gp, multidrug resistance proteins (MRP) (11), breast cancer resistance protein (BCRP) etc. on the luminal side of the BBB and degrading ecto- or endo-enzymes of the cytoplasm of endothelial cells prior to penetration into the brain (12). SLNs composed of biodegradable saturated lipids like HSPC are found to be biocompatible (13, 14) and prolong blood circulation life because of enhanced *in vivo* stability (15, 16). Pioneering characteristics of SLNs also extend many advantages such as controlled drug release (17), drug targeting and low biotoxicity, high drug payload, easy scale up, and amenability to sterilization (18, 19). But, they could not target the site of infection effectively due to lack of specificity (20, 21). There are number of approaches for surface modification of SLNs to enhance brain drug delivery including surface modification with hydrophilic polymers such as poloxamer (BBB disruption and Pgp efflux reversal) and polyethylene glycol (stealthing) which may be coupled with BBB specific ligands such as transferrin, peptides, and monoclonal antibodies etc. (22). To achieve enhanced localization, lactic acid conjugated SLN loaded with ALB-PRD (SLN-LA) were developed and studied for targeting potential in which LA facilitates SLNs transport via MCT-1/2/3 to the brain cells (15, 23). So, such fabricated SLNs could decrease dose, dose frequency and severe side effects of both drugs leading to enhanced safety and efficacy, and could be a promising tool for effective management of NCC. The overall view of strategy is depicted in Fig. 1.

MATERIALS AND METHODS

Materials

ALB and PRD were procured as gift samples from Mino Pharma and Sain Medicaments (Hyderabad, Andhra Pradesh, India) and Synmedic Laboratories, (Faridabad, Haryana, India), respectively. HSPC was benevolently obtained from Lipoid (Ludwigshafen Am Rhein, Germany). Fluorescein isothiocyanate (FITC), Triton X-100, Stearylamine (SA), DL-lactic acid (LA), 1-ethyl-3-(3-dimethylaminopropyl) carbodimide (EDC), N-Hydroxysulfosuccinimide (Sulfo-NHS), and Sephadex G-50 were purchased from Sigma Chemicals (St Louis, MO, USA). Tristearin and dialysis membrane (MWCO, 13KDa) were purchased from Himedia (Mumbai, Maharashtra, India). Nylon membrane filters were procured from Millipore (Bangalore, Karnataka, India). All other reagents and solvents used were of analytical grade unless stated otherwise. Double distilled water (DDW) was used throughout the study.

Methods

Drug-Drug Interaction Study

X-ray diffraction (XRD) patterns for ALB, PRD and their mixture (1:1) were recorded on a XPERT-PRO powder XRD using Ni-filtered CuK_{α} radiation (40 kV, 30 mA). The instrument was operated in the continuous scan mode at the angle of 2θ ranges 2–50°C with a speed of 5 mm/2 cm/2θ (IICT, Hyderabad, Andhra Pradesh, India). The graphical representation of XRD patterns were generated using PCPDF Win software (Japan).

Preparation of SLN

SLN were prepared using modified solvent injection method reported by Schubert *et al.* (2003) with slight modifications (24). In brief, tristearin, HSPC, stearylamine and drugs (ALB-PRD) were dissolved in the ethanol (5 mL) in a definite molar ratio with the aid of heat (60±1°C). Then, this organic phase (i.e., ethanolic solution of lipids and drugs) was injected into pre-warmed (60±1°C) aqueous phase (Tween 80: PBS pH 7.4, 1: 40) with continuous mechanical stirring (Remi Instruments, Mumbai, Maharashtra, India) at 2500 rpm for 45 min on thermostat mode. The resulting lipid suspension was sonicated using Probe sonicator (Lark innovative technology, Chennai, Tamil Nadu, India) to obtain SLN (Fig. 1). FITC was loaded using similar steps except drugs were replaced with FITC for carrying out fluorescent studies.

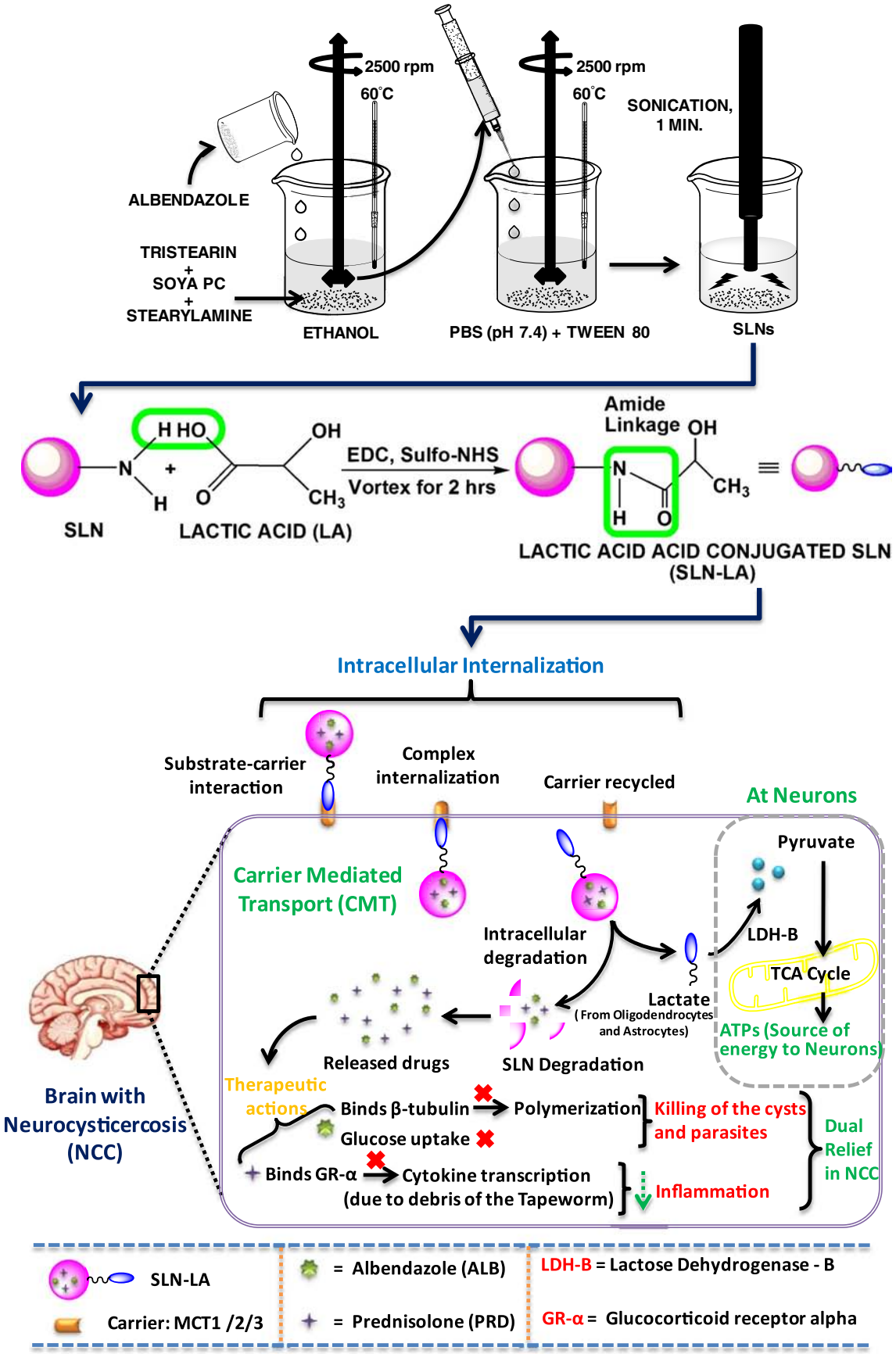

Fig. 1 Complete overview of the strategy.

Conjugation of SLN with LA

Before coupling the LA, its -OH group was protected using benzyl chloride and powdered KOH (25). The coupling of developed SLN with the –OH protected LA (OLA) was performed using carbodiimide chemistry i.e., coupling of activated carboxylic group of OLA with the amine group of SA of SLN in presence of EDC. Briefly, LA with pre-activated -COOH group using sulfo-NHS was dissolved in minimum quantity of PBS (pH 7.4) followed by dispersing it into 1.0 mL SLN. EDC (10 mg) was then added to above mixture followed by vortex for 2 h at room temperature. After adding a little quantity of ethanol, the mixture was subjected to hydrogenation in the presence of Pd–C (Palladium-Carbon) for the cleavage of protected –OH group (26). Unbound LA was removed by passing the formulation through Sephadex G-50 mini column. Conjugation was confirmed using FTIR and ^{1}H-NMR spectroscopic analysis.

Surface Charge, Size and Size Distribution

The zeta potential, average particle size and size distribution (polydispersity index, PDI) of SLNs were measured using Zetasizer (DTS ver.4.10, Malvern Instruments, England). The sample dispersion was diluted with DDW (1: 9*v*/*v*).

Particle Shape and Surface Morphology

A drop of the sample (SLNs) was placed on a carbon coated copper grid to leave a thin film on the grid. Before the film dried on the grid, the film was negatively stained with 1% phosphotungstic acid. The grid was air dried thoroughly and investigated under a transmission electron microscope (Philips CM 10, Netherlands) at suitable magnification.

For investigation of surface morphology, the samples were prepared by lightly sprinkling the SLNs powder on a double adhesive tape being stuck on an aluminium stub. The stubs were then coated with gold (thickness ~ 300 Å) using a sputter coater and examined under a scanning electron microscope (LEO 435 VP, Eindhoven Netherlands) at 30 kV.

Percent Entrapment Efficiency (%EE)

Entrapment efficiency of SLNs was determined using Sephadex G-50 mini column technique (27). Free drugs (ALB-PRD) were removed from SLNs using Sephadex G-50 mini column with centrifugation at 2000 rpm for 2 min. SLNs in void volume were then collected and disrupted using 0.1% Triton X-100. The amounts of entrapped drugs were analyzed using HPLC (Shimadzu Model-SPD-M20A, Kyoto, Japan). Mobile phase comprised of methanol–water (80:20) was run on Phenomenex Luna C-18(2) column (4.6 mm × 250 mm, dp = 5 μm; Hyderabad, India) in isocratic mode at 1 mL/min for simultaneous analysis of the two drugs using PDA detector (240 nm). The percent drug(s) entrapment efficiency was calculated separately using given formula:

$$\% EE = \left(W_f \Big/ W_i\right) \times 100$$

Where, W_f is amount of drug entrapped andW_i is initial amount of drug.

Similarly, percent drug loading (%DL) was determined using the formula:

$$\% DL = \left(\frac{W_f}{W_f + W_L}\right) \times 100$$

Where, W_f is amount of drug loaded and W_L is weight of the lipids and other ingredients except drug used in preparation of SLNs.

In Vitro Drug Release

Using dialysis tube method, *in vitro* drug release study was performed (28) for SLNs free from unbound drugs. SLNs (5 mL) taken in dialysis tube (MWCO, 13 KDa) were placed in a beaker containing 1 M methanolic formic acid in PBS (pH 7.4) at 1 : 25 (*v*/*v*). The release medium was continuously stirred (100 rpm) at 37 ± 1°C. Samples were withdrawn at definite time points up to 48 h and replenished with same volume of fresh medium every time. Samples were then analyzed for percent drugs release using HPLC method as stated before.

In Vitro Trans-Endothelial Transport Study

Brain capillary endothelial cells (BCECs) and astrocyte cells (ACs) were co-cultured 2–3 (× 10^5) cells/well on the lower side as well as upper side, respectively in polycarbonate 24 well cell culture insert with microporous PET membrane (D = 1 μm). The cells were cultured in 10% CO_2 for consecutive 7 days at 37°C to get 100% confluency. 250 μL of plain drugs (ALB-PRD), SLN, SLN-LA and free LA (1 mg/mL) + SLN-LA in Ringer-HEPES solution were added to different wells of the luminal compartment. At various time points, cells in the abluminal side were isolated and disrupted using Triton X-100 (5%; 250 μL) followed by centrifugation (1000 × g; 30 min). The supernatant was withdrawn and concentration of drugs was measured using HPLC method as discussed before.

In vitro permeability coefficients of the formulations (P) were obtained from the slope of the linear plot of formulation flux into the receiver chamber over time according to the following equation:

$$\mathbf{P} = \mathbf{Flux} \Big/ \left(\mathbf{C_{D,t}.A}\right) = \left(\mathbf{M_{R,\,t}} \Big/ \mathbf{t}\right) \Big/ \left(\mathbf{C_{D,t}.A}\right)$$

where $C_{D,t}$ is the concentration of the compound in the donor chamber at time t, $M_{R,t}$ is the amount of compound in the

receiver chamber at time t, and A is the surface area of the membrane exposed between the side-by-side chamber (0.636 cm^2).

In Vivo Studies

The protocol to perform *in vivo* studies comprising serum – drug profile and organ distribution study, fluorescent microscopy and hematological toxicity studies was duly approved by the Institutional Animal Ethical Committee of Dr. H. S. Gour University, Sagar, MP (Protocol No: Animal Eths. Comm./10/9).

Serum – Drug Profile and Organ Distribution Study

Albino rats (Wistar Strain) of either sex (110–120 g) were maintained on standard diet and water. Albino rats were divided into four groups having 9 rats of either sex in each group (4×9), in which the first group (Av. Wt. 116.7 g) served as a control. The second group (Av. Wt. 115.2 g) received free drugs solution (6 mg/kg, ALB; 1 mg/kg, PRD) whereas third (Av. Wt. 118.9 g) and fourth (Av. Wt. 110.4 g) groups were given SLN and SLN-LA, respectively. They were fasted overnight before administration of dose. The formulations were administered in rats via intravenous route through tail vein. After administration of formulations, three rats from each group was sacrificed after 0.5, 4, and 24 h. Blood samples were collected through cardiac puncture and stored well in heparin coated vials. Different vital organs i.e., kidney, liver, spleen and brain were isolated and dried with tissue paper and weighed. The organs were excised and homogenized in ortho phosphoric acid (2 mL, 0.4%) in methanol-PBS (pH 7.4) mixture (50:50) (29). The organic extracts were separated by centrifugation at 5000 rpm for 10 min and filtered through 0.45 μm nylon membrane filter. The percent drugs recovered was quantified using HPLC method as stated before. The various pharmacokinetic parameters were calculated using Thermo Kinetica Version 5.0 – Trail Version (Thermo Fisher Scientific Inc.).

Fluorescent Microscopy

The FITC loaded SLNs were administered to albino rats intravenously through tail vein. Rats were sacrificed after 4 h and brain was isolated. It was cut into small pieces and washed in Ringer's solution with subsequent drying using tissue paper. Dried pieces of the brain were fixed in Carnay's fluid (absolute alcohol: chloroform: glacial acetic acid, 3.5:1:0.5). Then, it was subjected to dehydration and embedded in paraffin followed by microtomy. The sections were observed under the fluorescent microscope (TE 2000, Nikon, Japan) at excitation and emission wavelengths of 495.0 and 520.0 nm, respectively.

Hematological Toxicity

Albino rats (Wistar Strain) of either sex (110–120 g) were used for determination of hematological parameters. First group of animals was kept as control. Plain drugs solution (second group), SLN (third group), and SLN-LA (fourth group) were administered intravenously in a dose equivalent (6 mg/kg, ALB; 1 mg/kg, PRD) daily up to a week. For hematological toxicity, the total white blood corpuscles (WBC), red blood corpuscles (RBC), platelets count and hemoglobin (Hb) content

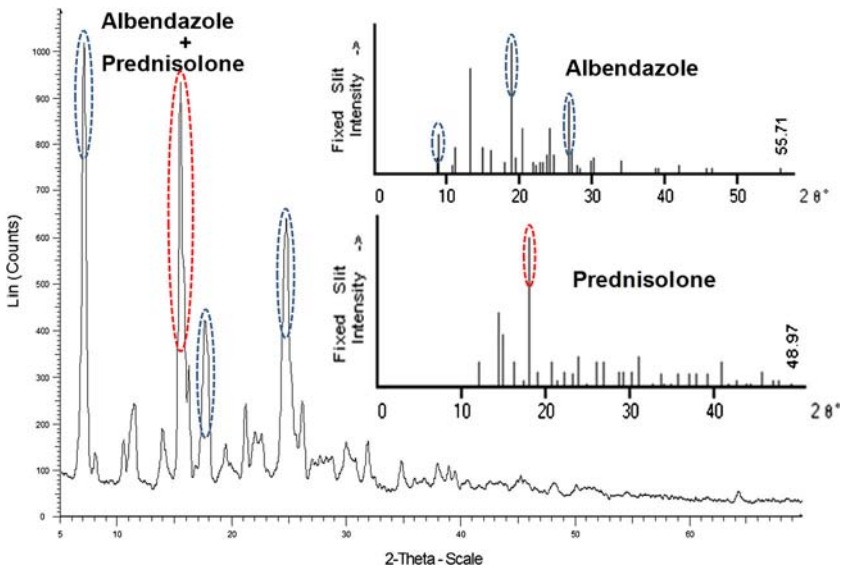

Fig. 2 XRD patterns of ALB, PRD and their mixture (1:1). Color highlights show individual contributions.

Table I Characteristic Features of SLNs

Formulation code	Composition (molar ratio)	Zeta potential (mV)	Particle Size (nm)	Average PDI	% EE		% DL	
					ALB	ALB	ALB	PRD
SLN	Tristearin : HSPC : SA : ALB : PRD (25 : 25 : 2.5 : 1 : 6)	− 25.3 ± 1.2	95.4 ± 0.9	0.265	73.6 ± 0.8	88.1 ± 1.0	78.3 ± 1.7	74.4 ± 1.8
SLN–LA	Tristearin : HSPC : SA : ALB : PRD : LA (25 : 25 : 2.5 : 1 : 6 : 1)	− 23.6 ± 0.5	100.2 ± 1.1	0.376	62.2 ± 0.4	77.9 ± 0.7	70.2 ± 0.9	70.8 ± 2.1

Values represent Mean ± SD ($n = 5$)

were determined on 8th day using a semi-automated blood cell counter with digital display (Sysmex cc-130, Toa Medical Electronics Ltd., Japan).

Statistical Analysis

All results were expressed as mean ± standard deviation (SD) & statistical analysis was performed with NCSS 2007 Version 07.1.14 (Utah, USA). *In vitro* drugs release model kinetics was analyzed using Sigma Plot for Windows Version 11.0 (wpcubed GmbH, Germany). All pharmacokinetic parameters were determined using Thermo Kinetica Version 5.0 – Trail Version (Thermo Fisher Scientific Inc.). A difference with $p \leq 0.05$ (i.e., 5%, level of significance) was considered to be statistically significant.

RESULTS

The XRD patterns (Fig. 2) of ALB, PRD and their physical mixture (1:1) were investigated using PCPDFWIN software (Japan). The individual XRD graph of ALB and PRD showed crystalline peaks prominent at 2θ value of 28.2 and 18.3° at intensities of 55.71 and 48.97, respectively. The mixture of ALB-PRD showed the characteristic peaks of both the drugs simultaneously, thus indicating no interaction between these two drugs and retention of the crystalline forms of both.

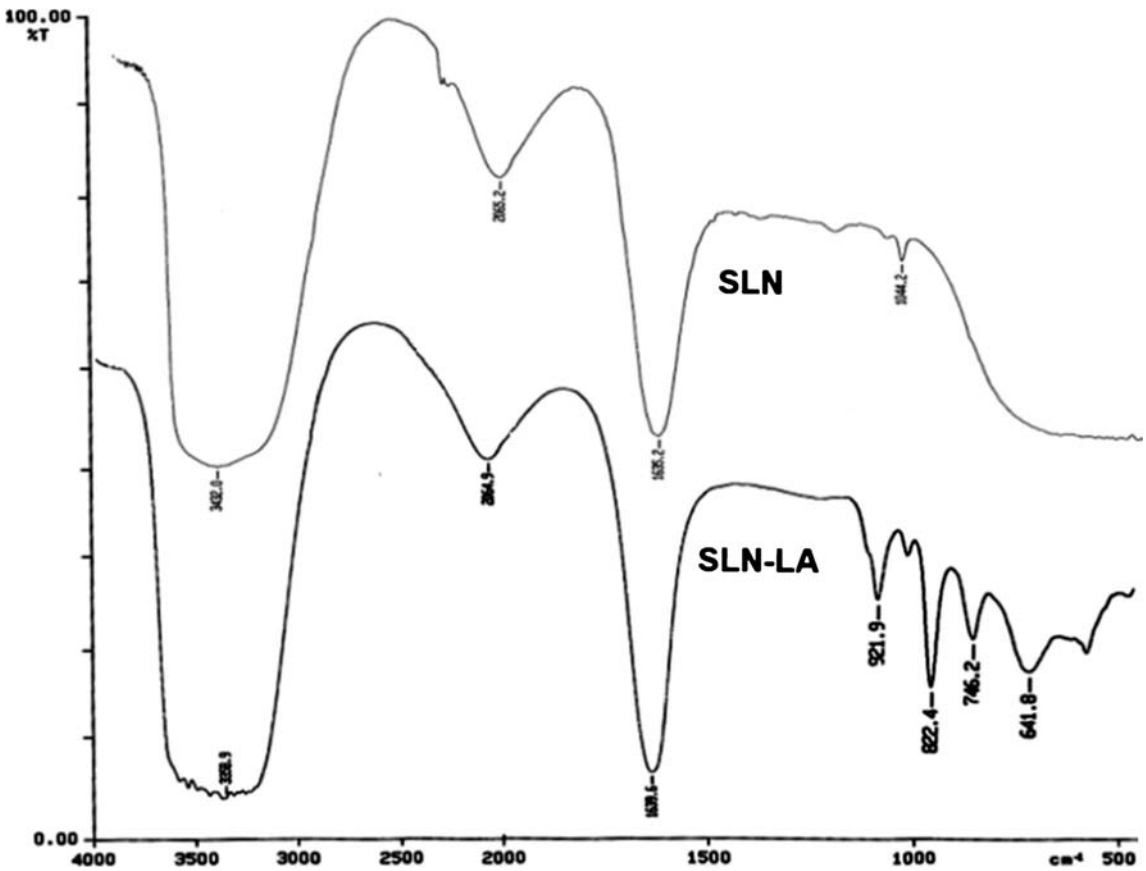

Fig. 3 FTIR spectra of SLN and SLN–LA.

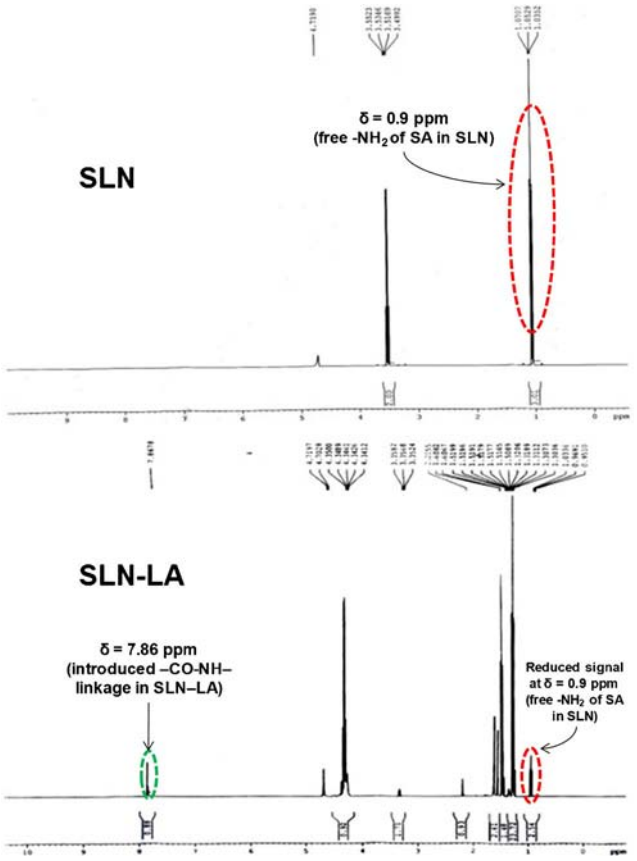

Fig. 4 ^{1}H-NMR spectra of SLN and SLN-LA (Encircled signals highlight characteristic contributions).

SLNs prepared from tristearin, HSPC, tween 80, SA, LA and drugs (ALB-PRD) using modified ethanol injection method possessed various characteristic features which have been summarized in Table I. FTIR and ^{1}H-NMR based comparative spectral analysis confirmed coupling with introduction of amide linkage in SLN-LA (Figs. 3 and 4). The IR spectrum of SLN–LA showed peaks at 3358.9 and 1639.6 cm^{-1} which indicated the presence of N-H stretch and C=O stretch in amide, respectively whereas SLN showed peaks at 3432.0 and 1635.2 cm^{-1} characteristic of N-H stretching and bending of amine group, respectively. The ^{1}H-NMR spectra of SLN showed δ=0.9 ppm (protons of free amine group in SLN) and δ=7.86 ppm in SLN-LA that depicted proton of amide bond (−CO-NH–). Figure 5 showed TEM and SEM images of SLN and SLN-LA.

Drugs released from SLNs were studied using dialysis tube method. The results indicated that the drugs release from SLNs was sustained for more than 48 h. After 48 h, it was 62.98±0.82 and 61.25±0.91% for ALB and PRD from SLN, respectively whereas SLN-LA showed 53.27±0.77 and 50.51±0.86% release of ALB and PRD, respectively (Fig. 6).

Transcytosis capability of free ALB-PRD, SLN, SLN-LA and free LA (1 mg/mL) + SLN-LA was studied on a co-culture of BCECs and ACs (Fig. 7). Their permeability coefficients ($\times 10^{-6}$ cm/s) were found to be 0.6, 1.8, 24, and 1.7, respectively. It was observed that SLN was showing 3 folds higher transcytosis as compared to free ALB-PRD and SLN-LA was exhibiting 13.33 folds and 40 folds higher transcytosis as compared to SLN and free ALB-PRD, respectively. Moreover, in case of free LA (1 mg/mL) + SLN-LA, transcytosis was similar to SLN.

In case of plain drugs solution, around 50% of dose (ALB-PRD) was recovered from serum after 0.5 h but no drug was detected after 24 h. Moreover, there was only ~15 and ~10% of dose (ALB-PRD) recovered from serum after 24 h in case of SLN and SLN-LA, respectively (Fig. 8). Pharmacokinetic parameters (Table II) revealed increased $AUC_{0\text{-}t}$ (μg/μL×h) and $AUMC_{0\text{-}t}$ (μg/μL×h^2) for both of the drugs in case of SLNs compared to plain drugs solution i.e., ~3 folds and ~16 folds higher, respectively. There was reduced Cl_{last} (Clearance

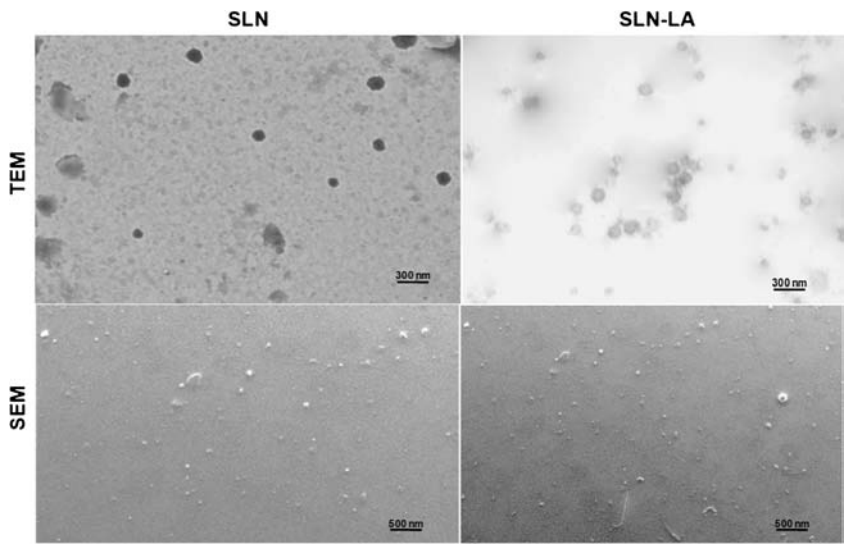

Fig. 5 TEM and SEM images of SLN and SLN-LA.

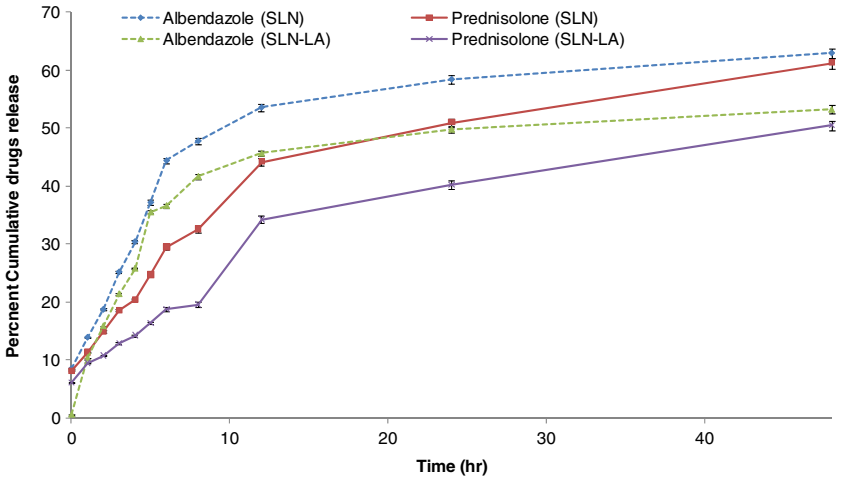

Fig. 6 *In vitro* percent cumulative drugs release in PBS (pH 7.4) from SLNs (Mean ± SD, $n = 6$; $p \leq 0.05$).

at last time point) in case of SLNs (2 folds lower) compared to plain drugs solution. Amount of drugs accumulated in the vital organs following *i.v.* administration of various formulations has been summarized in Table III.

Fluorescence microscopy was performed to observe the qualitative uptake potential of SLNs in brain (Fig. 9).

Noticeable decrease in blood cells count such as WBC count, RBC count, Hb content, platelet count were found after *i.v.* administration of free drug solutions for 7 days but there was less significant difference in blood cells count in case of SLN. Moreover, SLN-LA showed no hematological implications. The significant difference was observed between free ALB-PRD Vs SLN and SLN-LA (Table IV).

DISCUSSION

Combinatorial approach was successfully employed with targeting technology to fabricate SLNs using post insertion technique (30). Coupling of SLN with LA was performed using carbodiimide chemistry in which carboxylic group of LA was conjugated to amine group of SA of SLN with the help of EDC as a coupling agent. Protection of hydroxyl group of LA was necessary to prevent unwanted by products and increase yield of SLN-LA (25). TEM revealed that SLNs were spherical in shape, nanometeric in size and maintained their structural integrity. SEM confirmed the smoothness of SLN's surface even after coupling with LA. There was slight increase in size of SLN-LA as compared to SLN due to surface oriented LA (13).

PDI showed narrow size distribution of SLNs and homogeneity. The negative zeta potential of SLN was accounted to negative charge of tristearin (31). The surface charge of SLN-LA was more negative as compared to SLN due to masking of positive charge of amine groups (SA) by LA during coupling. Drug entrapment was less in SLN-LA than SLN due to a bit leaching of the drugs during conjugation (32, 33). Drug loading in SLNs for ALB and PRD was more than 70% because of hydrophobic nature of drugs. *In vitro* drugs release showed slower drug release from SLN-LA due to the structural integrity

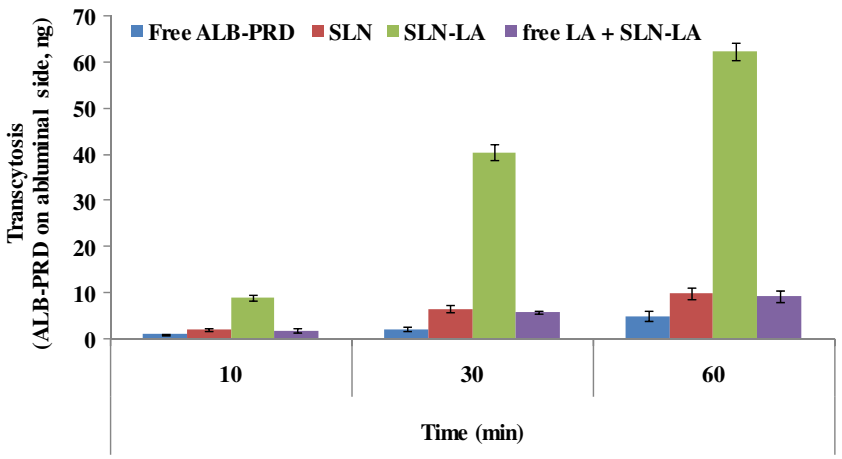

Fig. 7 Time dependent transcytosis of ALB-PRD across BCECs and ACs from free ALB-PRD, SLN, SLN-LA and free LA + SLN-LA (Mean ± SD, $n = 6$; $p \leq 0.05$).

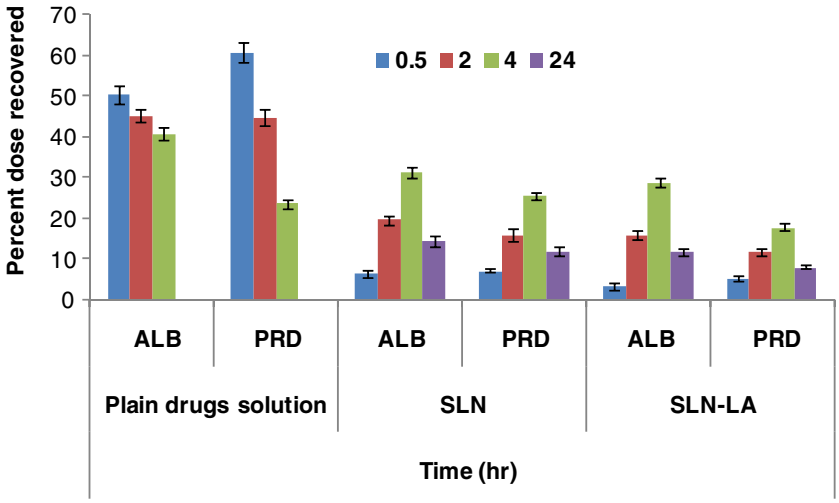

Fig. 8 Percent dose recovery in serum after *i.v.* administration of various formulations (Mean ± SD, $n = 6$; $p \leq 0.05$).

bestowed by coupled LA posing double-barrier effect to drugs to pass through (17).

Maximum transendothelial transport was observed in case of SLN-LA attributed to ability of LA conjugated SLN to undergo carrier-mediated transcytosis (MCT-1/2/3) across the BCECs and ACs. Transendothelial movement was less in case of free LA + SLN-LA due to competitive inhibition by free LA as substrate for MCTs. This further assures LA mediated transcytosis.

In serum profiles of drugs (ALB-PRD) solution, C_{max} was attained in 0.5 h as compared to SLN and SLN-LA accounted to availability of free drug from solution in serum while most of the drugs were entrapped in case of SLNs. After 24 h, the results obtained were in contrast to initial hours as drugs available from plain drugs solution got eliminated from serum due to metabolism in liver followed by faster clearance from the body while SLNs showed sustained release of drugs due to retardation in release posed by lipid matrix (17). Pharmacokinetic parameters showed enhanced $AUC_{0\text{-}t}$ and $AUMC_{0\text{-}t}$, and decreased Cl_{last} in case of SLNs compared to plain drugs solution that could be accounted to faster body clearance of free drugs from plain drugs solution and good drugs withholding capacity of SLNs, respectively.

Organ distribution profile revealed that no drugs were recovered in brain after administration of plain drugs solution even after 24 h due to presence of BBB and RES uptake of drugs from the liver and spleen (34). SLN provided 6–7% drugs to brain in 4 h because of lipidic nature compatible with BBB but also partly subjected to RES uptake (35). Interestingly, SLN-LA successfully traversed BBB with 15-18% drugs in

Table II Pharmacokinetic Parameters for Plain Drugs (ALB-PRD) Solution, SLN and SLN-LA

Parameter (Unit)	Formulations					
	Plain drugs solution		SLN		SLN-LA	
	ALB	PRD	ALB	PRD	ALB	PRD
C_{max} (μg/mL)	50.45	60.83	31.45	21.49	28.81	17.9
T_{max} (h)	0.5	0.5	4	4	4	4
$AUC_{0\text{-}t}$ ($\mu g/\mu L \times h$)	183.48	178.01	512.00	420.19	443.38	292.473
$AUC_{0\text{-}\infty}$ ($\mu g/\mu L \times h$)	870.53	267.67	NA	NA	NA	NA
$AUMC_{0\text{-}t}$ ($\mu g/\mu L \times h^2$)	352.23	295.03	5768.64	4725.35	4971.04	3253.03
$AUMC_{0\text{-}\infty}$ ($\mu g/\mu L \times h^2$)	14,689.4	983.52	NA	NA	NA	NA
$t_{1/2}$ (h)	11.6919	2.55	NA	NA	NA	NA
HVD (h)	NA	NA	20.36	20.91	17.85	20.1564
MRT (h)	16.87	3.67	11.26	11.24	11.21	11.12
Cl_{last} ($\mu L/h$)	40.93	23.71	14.5	11.98	11.9	8.1

NA Not applicable; Probability $p \leq 0.05$; SD < 5%

Abbreviations: C_{max} peak plasma concentration, T_{max} time to reach peak plasma concentration, *AUC*, area under plasma drug concentration over time curve, *AUMC* area under the first moment curve, $t_{1/2}$ elimination half life, Cl_{last} Clearance at last time point, *MRT* mean residence time, *HVD* half value duration

Table III Organ Distribution of Drugs After *i.v.* Administration of Plain Drugs Solution, SLN and SLN-LA

Time (h)	Percent drugs recovered from plain drugs solution							
	Brain		Liver		Kidney		Spleen	
	ALB	PRD	ALB	PRD	ALB	PRD	ALB	PRD
0.5	ND[a]	ND	24.82 ± 0.42	25.94 ± 0.39	13.26 ± 0.16	10.25 ± 0.15	8.37 ± 0.24	6.26 ± 0.28
4	ND	ND	13.05 ± 1.21	16.94 ± 0.99	18.91 ± 0.34	12.83 ± 0.59	4.62 ± 0.72	3.64 ± 0.68
24	ND	ND	6.21 ± 0.95	4.87 ± 1.12	5.32 ± 1.19	5.92 ± 0.98	1.71 ± 0.09	1.01 ± 0.21
Time (h)	Percent drugs recovered from SLN							
	Brain		Liver		Kidney		Spleen	
	ALB	PRD	ALB	PRD	ALB	PRD	ALB	PRD
0.5	0.78 ± 0.03	0.65 ± 0.05	20.05 ± 0.18	15.82 ± 0.13	7.82 ± 0.21	5.94 ± 0.11	1.21 ± 0.02	1.16 ± 0.03
4	6.65 ± 0.09	6.19 ± 0.07	9.87 ± 0.32	7.14 ± 0.53	10.95 ± 0.61	8.29 ± 0.21	2.51 ± 0.41	2.46 ± 0.82
24	5.16 ± 0.12	4.82 ± 0.10	2.08 ± 1.62	1.38 ± 1.01	4.23 ± 0.91	6.23 ± 0.75	1.01 ± 0.65	0.99 ± 0.91
Time (h)	Percent drugs recovered from SLN-LA							
	Brain		Liver		Kidney		Spleen	
	ALB	PRD	ALB	PRD	ALB	PRD	ALB	PRD
0.5	10.79 ± 0.22	8.92 ± 0.19	19.37 ± 1.24	18.48 ± 1.10	11.54 ± 0.92	16.18 ± 0.94	0.85 ± 1.03	0.76 ± 1.02
4	18.54 ± 0.43	15.73 ± 0.39	8.92 ± 0.59	9.67 ± 0.48	2.89 ± 0.61	5.32 ± 0.65	0.96 ± 0.96	0.83 ± 0.91
24	7.63 ± 0.31	5.21 ± 0.24	2.65 ± 0.93	1.98 ± 0.83	1.48 ± 0.86	0.95 ± 0.79	ND	ND

Values represent Mean ± SD ($n = 6$)

[a] *ND* Not detected

the brain i.e., 3 fold higher brain uptake as compared to SLN accounting to MCT facilitated uptake and least accumulation in other vital organs (36). This was again assured with the fluorescence photomicrographs that showed the qualitative localization patterns of the SLNs in brain where FITC loaded SLN-LA showed enhanced fluorescence density as compared to SLN due to the presence of MCTs which facilitate lactic acid transport to the brain (37, 38).

In hematological studies, evident decrease in blood cells count such as WBC count, RBC count, Hb content, platelet count was observed in case of free drug solutions but there were lesser hematological implications in case of SLNs. This could be due to the direct contact of free drugs with blood cells but when drugs were encapsulated in SLNs it led to reduced hematological toxicity. Moreover, there were almost no changes in blood cells count in case of SLN-LA as compared to control group due to target specificity of SLN-LA leading to selective drugs delivery to brain and very less amount of drugs got leached out in systemic circulation (39).

CONCLUSION

On the basis of above findings, developed lactic acid conjugated SLN could be a promising tool to treat NCC effectively by dual drug delivery to the brain. Since, NCC being chronic in nature requires long term therapy, SLN-LA not only targeted brain but also offered sustained and prolonged release of these synergistic drugs in which albendazole kills the parasites and prednisolone alleviates inflammation due to deceased parasites in the brain. Hence, this targeted brain delivery was found to be safe and efficacious for the management of NCC.

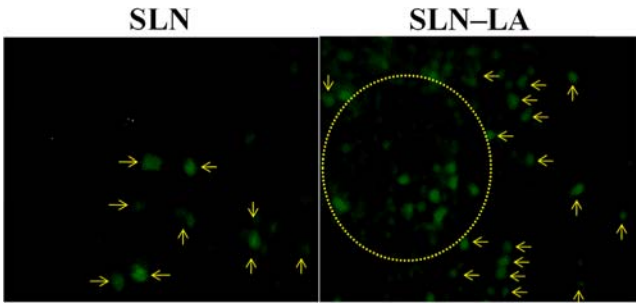

Fig. 9 Fluorescent uptakes of SLNs in the brain after 4 h.

Table IV Hematological Parameters After *i.v.* Administration of Plain Drugs Solution, SLN & SLN-LA

Groups	WBC ($\times 10^3/\mu L$)	RBC ($\times 10^3/\mu L$)	Hb (g/dL)	Platelet count ($\times 10^3/\mu L$)
Control	8.5 ± 1.7	9.6 ± 0.3	16.9 ± 1.1	1000.2 ± 30.5
Free ALB-PRD	3.5 ± 0.4	6.7 ± 1.2	10.1 ± 1.6	825.1 ± 31.7
SLN	7.0 ± 0.8	8.9 ± 0.5	15.5 ± 0.9	972.1 ± 34.5
SLN-LA	8.5 ± 1.5	9.5 ± 0.9	16.8 ± 0.3	1000.1 ± 33.4

Values represent Mean ± SD ($n = 6$, $p \leq 0.05$)

ACKNOWLEDGMENTS AND DISCLOSURES

Authors are thankful to Mino Pharma and Sain Medicaments (Hyderabad, India) and Synmedic Laboratories, Faridabad (Haryana, India) for providing gift samples of drugs. We wish to acknowledge the support of Lipoid (Ludwigshafen Am Rhein, Germany) for rendering gift samples of lipids. The authors are also thankful to AIIMS, New Delhi for carrying out TEM and SEM studies. Authors namely Mr. Ankit Jain and Ms. Pooja Hurkat are highly obliged to Council of Scientific and Industrial Research (New Delhi, India) for rendering Senior Research Fellowship (SRF). The authors declare no competing financial interest and they alone are responsible for the content and writing of the manuscript.

REFERENCES

1. Soteloand J, Del Brutto OH. Review of neurocysticercosis. Neurosurg Focus. 2002;12:1–7.
2. Garcia HH, Lescano AG, Lanchote VL, Pretell EJ, Gonzales I, Bustos JA, *et al.* Pharmacokinetics of combined treatment with praziquantel and albendazole in neurocysticercosis. Br J Clin Pharmacol. 2011;72:77–84.
3. Abbottand NJ, Romero IA. Transporting therapeutics across the blood–brain barrier. Mol Med Today. 1996;2:106–13.
4. Löscherand W, Potschka H. Drug resistance in brain diseases and the role of drug efflux transporters. Nat Rev Neurosci. 2005;6:591–602.
5. Tsuji A. Small molecular drug transfer across the blood–brain barrier via carrier-mediated transport systems. NeuroRx. 2005;2:54–62.
6. Kim MH, Maeng HJ, Yu KH, Lee KR, Tsuruo T, Kim DD, *et al.* Evidence of carrier-mediated transport in the penetration of donepezil into the rat brain. J Pharm Sci. 2010;99:1548–66.
7. Matthaiou DK, Panos G, Adamidi ES, Falagas ME. Albendazole versus praziquantel in the treatment of neurocysticercosis: a meta-analysis of comparative trials. PLoS Negl Trop Dis. 2008;2:e194.
8. Cruz I, Cruz M, Carrasco F, Horton J. Neurocysticercosis: optimal dose treatment with albendazole. J Neurol Sci. 1995;133:152–4.
9. Carpio A, Kelvin EA, Bagiella E, Leslie D, Leon P, Andrews H, *et al.* Effects of albendazole treatment on neurocysticercosis: a randomised controlled trial. J Neurol Neurosurg Psychiatry. 2008;79:1050–5.
10. Chattopadhyay N, Zastre J, Wong H-L, Wu XY, Bendayan R. Solid lipid nanoparticles enhance the delivery of the HIV protease inhibitor, atazanavir, by a human brain endothelial cell line. Pharm Res. 2008;25:2262–71.
11. Löscherand W, Potschka H. Blood–brain barrier active efflux transporters: ATP-binding cassette gene family. NeuroRx. 2005;2:86–98.
12. Brasnjevic I, Steinbusch HW, Schmitz C, Martinez-Martinez P. Delivery of peptide and protein drugs over the blood–brain barrier. Prog Neurobiol. 2009;87:212–51.
13. Kharya P, Jain A, Gulbake A, Shilpi S, Jain A, Hurkat P, *et al.* Phenylalanine-coupled solid lipid nanoparticles for brain tumor targeting. J Nanoparticle Res. 2013;15:1–12.
14. Rai A, Jain A, Jain A, Jain A, Pandey V, Chashoo G, et al. Targeted SLNs for management of HIV-1 associated dementia. Drug Dev Ind Pharm. 2014;1–7.
15. Redzic Z. Molecular biology of the blood–brain and the blood-cerebrospinal fluid barriers: similarities and differences. Fluids Barriers CNS. 2011;8:1–25.
16. Mamta Bishnoi AJ, Pooja Hurkat, Jain SK. Aceclofenac-loaded chondroitin sulfate conjugated SLNs for effective management of osteoarthritis. J Drug Target. 2014;1–8.
17. MuÈller RH, MaÈder K, Gohla S. Solid lipid nanoparticles (SLN) for controlled drug delivery–a review of the state of the art. Eur J Pharm Biopharm. 2000;50:161–77.
18. Müller R, Hildebrand G, Nitzsche R, Paulke B-R. Zetapotential und Partikelladung in der Laborpraxis. PAPERBACK APV. 1996;37.
19. Lim SB, Banerjee A, Önyüksel H. Improvement of drug safety by the use of lipid-based nanocarriers. J Control Release. 2012;163:34–45.
20. Kaur IP, Bhandari R, Bhandari S, Kakkar V. Potential of solid lipid nanoparticles in brain targeting. J Control Release. 2008;127:97–109.
21. Blasi P, Giovagnoli S, Schoubben A, Ricci M, Rossi C. Solid lipid nanoparticles for targeted brain drug delivery. Adv Drug Deliv Rev. 2007;59:454–77.
22. Jain A, Jain SK. Brain Targeting Using Surface Functionalized Nanocarriers in human solid tumors. In: Singh B, Jain NK, Katare OP, editors. Drug nanocarriers. Houston: Series Nanobiomedicine Studium Press; 2014. p. 203–55.
23. Kennedyand KM, Dewhirst MW. Tumor metabolism of lactate: the influence and therapeutic potential for MCT and CD147 regulation. Future Oncol. 2010;6:127–48.
24. Schubertand M, Müller-Goymann C. Solvent injection as a new approach for manufacturing lipid nanoparticles–evaluation of the method and process parameters. Eur J Pharm Biopharm. 2003;55:125–31.
25. Kocienski PJ. Protecting groups. Thieme. 2005.
26. Greeneand TW, Wuts PG. Protection for the Hydroxyl Group, Including 1, 2-and 1, 3-Diols. 3rd ed. Protective Groups in Organic Synthesis; 1999 pp. 17–245.
27. Soppimath KS, Aminabhavi TM, Kulkarni AR, Rudzinski WE. Biodegradable polymeric nanoparticles as drug delivery devices. J Control Release. 2001;70:1–20.
28. Jain A, Gulbake A, Jain A, Shilpi S, Hurkat P, Jain SK. Dual drug delivery using "smart" liposomes for triggered release of anticancer agents. J Nanoparticle Res. 2013;15:1–12.
29. Truong Cong T, Faivre V, Nguyen TT, Heras H, Pirot F, Walchshofer N, *et al.* Study on the hydatid cyst membrane: permeation of model molecules and interactions with drug-loaded nanoparticles. Int J Pharm. 2008;353:223–32.
30. Souto EB, Fangueiro JF, Müller RH. Solid Lipid Nanoparticles (SLN™). Fundamentals of pharmaceutical nanoscience, Springer: 2013, pp. 91–116.
31. Paliwal R, Rai S, Vaidya B, Khatri K, Goyal AK, Mishra N, *et al.* Effect of lipid core material on characteristics of solid lipid nanoparticles designed for oral lymphatic delivery. Nanomedicine Nanotechnol Biol Med. 2009;5:184–91.
32. Bishnoi M, Jain A, Hurkat P, Jain SK. Aceclofenac-loaded chondroitin sulfate conjugated SLNs for effective management of osteoarthritis. J Drug Target. 2014;1–8.
33. Venkateswarluand V, Manjunath K. Preparation, characterization and in vitro release kinetics of clozapine solid lipid nanoparticles. J Control Release. 2004;95:627–38.
34. Manjunathand K, Venkateswarlu V. Pharmacokinetics, tissue distribution and bioavailability of nitrendipine solid lipid nanoparticles after intravenous and intraduodenal administration. J Drug Target. 2006;14:632–45.
35. Göppertand TM, Müller RH. Polysorbate-stabilized solid lipid nanoparticles as colloidal carriers for intravenous targeting of drugs

to the brain: comparison of plasma protein adsorption patterns. J Drug Target. 2005;13:179–87.
36. Kido Y, Tamai I, Okamoto M, Suzuki F, Tsuji A. Functional clarification of MCT1-mediated transport of monocarboxylic acids at the blood–brain barrier using in vitro cultured cells and in vivo BUI studies. Pharm Res. 2000;17:55–62.
37. Tamai I, Takanaga H, Ogihara T, Higashida H, Maeda H, Sai Y, *et al*. Participation of a proton-cotransporter, MCT1, in the intestinal transport of monocarboxylic acids. Biochem Biophys Res Commun. 1995;214:482–9.
38. Hertzand L, Dienel GA. Lactate transport and transporters: general principles and functional roles in brain cells. J Neurosci Res. 2005;79:11–8.
39. Agarwal A, Agrawal H, Tiwari S, Jain S, Agrawal GP. Cationic ligand appended nanoconstructs: a prospective strategy for brain targeting. Int J Pharm. 2011;421:189–201.